Thermal Storage Nanocapsules by Miniemulsion Polymerization

Maider García de Cortazar, Raquel Rodríguez

TECNALIA, Paseo Mikeletegi 2, E-20009 Donostia-San Sebastián, Spain
Correspondence to: R. Rodríguez (E-mail: raquel.rodriguez@tecnalia.com)

ABSTRACT: Paraffin wax was nanoencapsulated by miniemulsion polymerization. Low solid content batch polymerizations were carried out and the influence of paraffin wax/methyl methacrylate ratio on polymeriztion kinetics, phase change properties, and thermal stability were investigated. Paraffin concentration controls the nucleation mechanism and nanocapsules particle size. The latent heat capacity increases as the content of encapsulated paraffin wax increases. The maximum amount of encapsulated paraffin wax achieved under the experimental conditions was 60 wt %, presenting a latent heat capacity of 140.3 J/g. Moreover, the encapsulated systems present in all cases better thermal stability than pure paraffin wax. © 2012 Wiley Periodicals, Inc. J. Appl. Polym. Sci. 000: 000–000, 2012

INTRODUCTION

During the last decades, energy conservation has been on the rise and new sources for more efficient, ecologically friendly, and cost-effective ways to capture and store energy are being investigated.

In this regard, latent heat storage materials appear as an interesting alternative for thermal energy storage. These materials change state during what is called, a phase transition, and through this process heat energy is released or absorbed depending on the direction of the phase transition.[1] The main advantages of latent heat storage materials or simply phase change materials (PCMs) are those derived from the temperature control and the high heat storage capacity during the phase transition. Therefore, energy release/absorption takes place at almost constant temperature making the process easier to regulate, which is beneficial for the control of the surroundings temperature.[2] Besides, PCMs are also able to storage large amounts of heat at comparatively small temperature change. Consequently, their applications have been widely investigated, for example, as active or pumped coolants,[3] solar and nuclear heat storage systems, packed bed heat exchangers[4] and thermoregulated fibres, coatings, and foams.[5,6]

In most cases, PCM needs to be encapsulated to hold the liquid phase of the PCM, and thus to avoid PCM contact with the surroundings, which might harm the environment or change the composition of the PCM. Further on, the surface of the capsule acts as heat transfer surface. Since 1970, macroencapsulated and microencapsulated PCMs have been investigated,[7] however the latter has attracted special attention during the last years.[8]

Different organic PCMs have been microencapsulated by different processes such as *in situ* polymerization,[9–13] interfacial polymerization,[1,14] suspension polymerization,[15,16] complex coacervation, or spray drying.[17] The size of PCM capsule plays an important role because besides the containment of the liquid phase, the decrease of the size of the capsule improves the heat transfer to the surrounding, due to the large surface to volume ratio of the capsules and improves its cycling stability as phase separation is restricted to these small sized distances. Thus, the nanoencapsulation of PCMs provides many opportunities to study new frontiers to improve energy efficiently for many applications.

In this sense, miniemulsion polymerization has emerged as a promising polymerization strategy for the nanoencapsulation of water-insoluble PCM (paraffin wax, polyols), because monomer droplets are the main loci of particle formation and water-insoluble compounds can be nanoencapsulated.[18] Even though droplet nucleation has been controversial, several results show that nucleation of most of the droplets can be achieved at low solid content batch miniemulsion polymerizations.[19,20]

Therefore, miniemulsion polymerization is a convenient encapsulation technology to obtain nanocapsules. Fang et al.[21,22] studied the nanoencapsulation of *n*-octadecane with polystyrene shell. They studied the influence of polymerization factors, such as initiator, chain transfer agent, surfactant, and *n*-octadecane/styrene ratio, on the morphology and thermophysical properties of synthesized nanocapsules. Chen et al.[23] prepared poly(methyl methacrylate) (PMMA) nanocapsules containing *n*-dodecanol. They observe that the addition of 3% of polymerizable

Table I. Formulations Used in the Polymerizations

	Monomers[a]	Paraffin wax[a]	SA[a]	SDS[a]	Solids content[b] (%)	Initiator[a]
BM0	100	–	4	2	10	0.75 APS
BM5	100	5	4	2	10	0.75 APS
BM20	100	20	4	2	10	0.75 APS
BM40	100	40	4	2	10	0.75 APS
BM60	100	60	4	2	10	0.75 APS

BM: Batch reactions, [a]Relative weight amounts, [b]respect to the monomer.

emulsifier increases nanocapsules thermal storage capacity; however, above this percentage, thermal storage capacity is reduced. On the other hand, Zhang et al.[24] encapsulated *n*-octadecane using PMMA and polyethyl methacrylate, in their study they achieved an encapsulation efficiency of 89.5%.

The aim of this work is the nanoencapsulation by miniemulsion polymerization of a paraffin wax that presents a phase change transition at higher temperature that the ones mention on the literature (60°C, solid at room temperature). Among the possible polymeric shells, polymethylmethacrylate (PMMA) has been chosen because it presents good mechanical properties and good protection against outside environment.[25,26] The effect of the amount of encapsulated PCM on thermal storage properties and nanocapsules thermal stability was considered. In addition, its influence on polymerization rate, particle size, and particle size distribution (PSD) was discussed.

EXPERIMENTAL

Materials

Technical grade monomer MMA supplied by Aldrich was used without purification. A paraffin wax was used as PCM (RT60, Rubitherm); stearyl acrylate (SA, Aldrich) was used as a costabilizer; sodium dodecyl sulfate (SDS, Aldrich) was used as the surfactant. Ammonium persulfate (APS, Panreac) was used as initiator system. Distilled water was used throughout all the work.
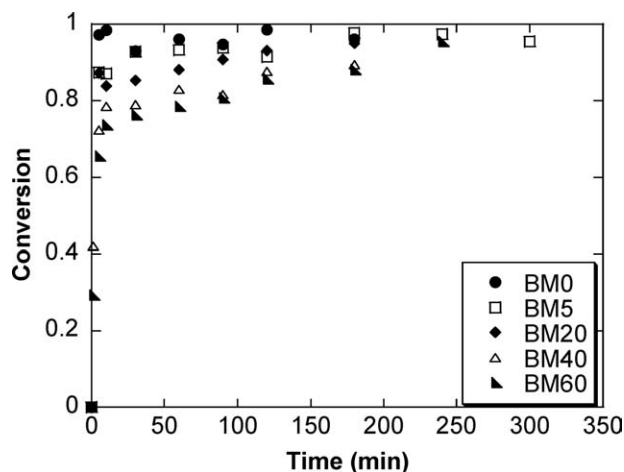
Figure 1. Evolution of conversion in batch miniemulsion polymerization with varying concentrations of Paraffin wax. ●BM0; □BM5; ◆BM20; △BM40; ◣BM60.

Nanoencapsulation

Miniemulsification. The organic phase was prepared by melting the paraffin wax (different paraffin wax content) and mixing it with the reactive costabilizer (SA, when used) and MMA at 60°C. The aqueous phase was prepared by dissolving the surfactant (SDS) in water. Both phases were mixed during 10 min using a magnetic stirrer at 1000 rpm at 60°C to keep the paraffin wax liquid. The coarse emulsion was sonified in a Sonoplus HD 2200 (250 W/L) during 20 min.

Polymerization Processes. Batch polymerizations were carried out in a 500 mL glass reactor equipped with reflux condenser, stirrer, sampling device, and nitrogen inlet. Reaction temperature was set constant by controlling the temperature of the fluid in the jacket by means of a thermostatic bath and a heat exchanger. The miniemulsion (10 wt % organic phase) was added to the reactor and kept under stirring and nitrogen atmosphere (12–15 mL/min). When the reaction temperature was reached, the initiator was injected.

All the reactions were carried out at 70°C. Samples were withdrawn at regular intervals, and the polymerization was short-stopped with hydroquinone. The conversions were determined gravimetrically. The conversion was calculated with respect to the monomer, namely the paraffin wax content was not taken into account. Table I presents a summary of the reactions.

Table II. Paraffin Wax Concentration Effect on Particle Population and Size Measured by AF4-MLS

Reference	Population radius (nm)	%Total	Media radius (nm)
BM0	10–18	96%	17.5 ± 0.5
	18–21	2%	
BM5	31–40	97%	37.0 ± 0.9
	40–52	3%	
BM20	49–63	81%	59.4 ± 3.6
	63–69	12%	
BM40	16–80	31%	137.4 ± 0.8
	80–189	69%	
BM60	83–247	76%	219.7 ± 0.8
	247–373	23%	
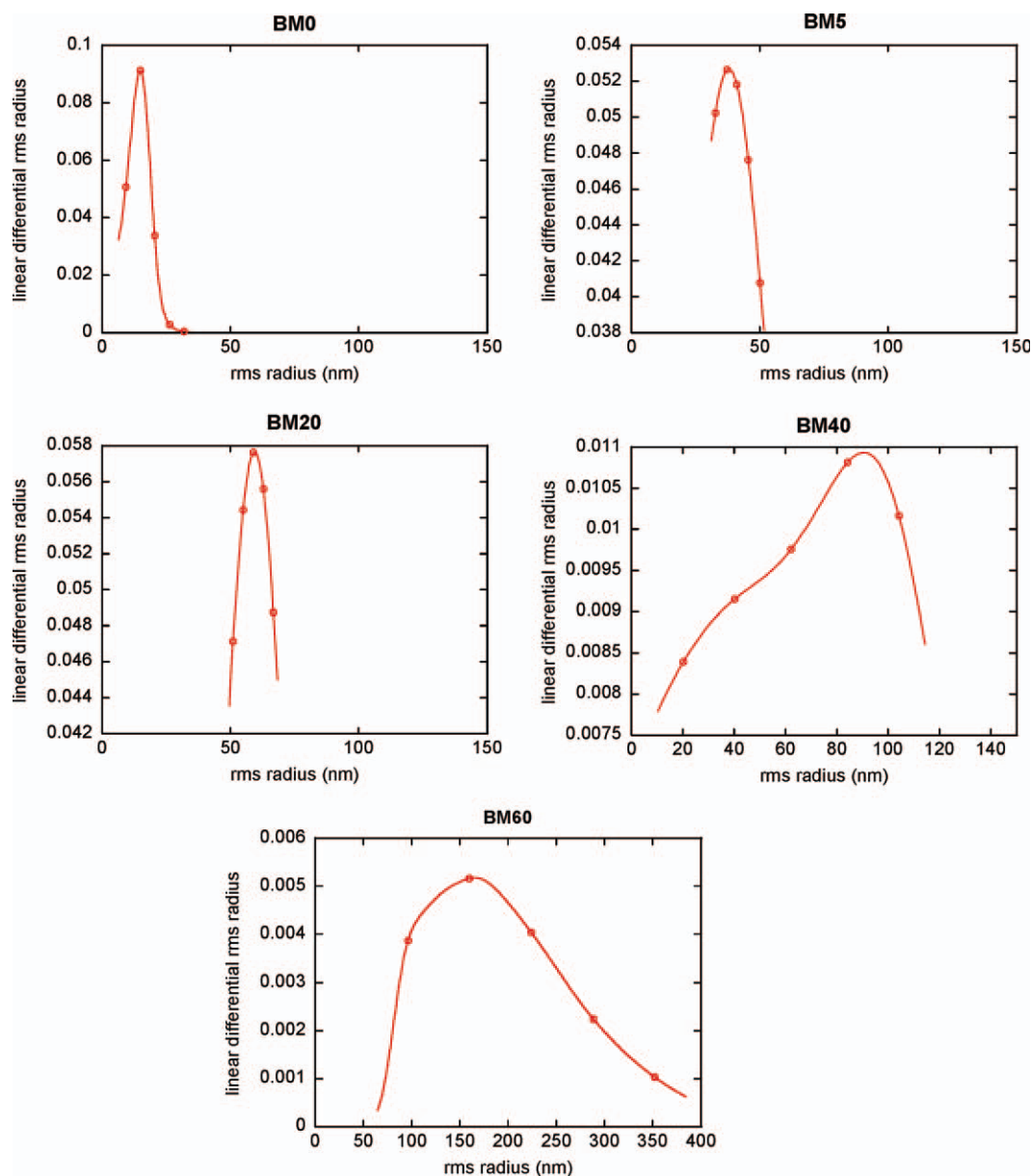
Figure 2. Evolution of PSD varying paraffin concentration. [Color figure can be viewed in the online issue, which is available at wileyonlinelibrary.com.]

Lyophilization. Particles were separated using a Lyophilizer (or freeze-dryer) Epsilon 2 (CHRIST). Samples were lyophilized at 0.63 mbar, −10°C during 4 days.

Nanocapsules Characterization
Particle Size and PSD. Particle size (dp) and PSD were measured by a AF4-MLS (WYATT). The equipment is based on the asymmetric flow field-flow fraction theory (ECLIPSE) coupled with multiangle light scattering detector which makes possible the determination of absolute molar mass and size of the fractionated molecules from AF4.

Differential Scanning Calorimetry. Nanoparticles energy storage capacity was measured by a differential scanning calorimetry (DSC) Q 100 (TA Instruments). Samples were weighted into aluminium pans and covers were sealed into place. An empty

pan was used as reference. Samples were heated at a constant rate of 10°C/min from −70°C to 100°C.

Scanning Electron Microscopy. Particle morphology was measured by scanning electron microscopy (SEM). Samples were

Table III. Paraffin Wax/MMA Ratio Effect on Particle Size and the Number of Particles

	Particle size (nm)	Np (part/L Latex)
BM0	35	5.8e18
BM5	74	5.98e17
BM20	118.8	1.45e17
BM40	274.8	1.06e16
BM60	439.4	2.47e15
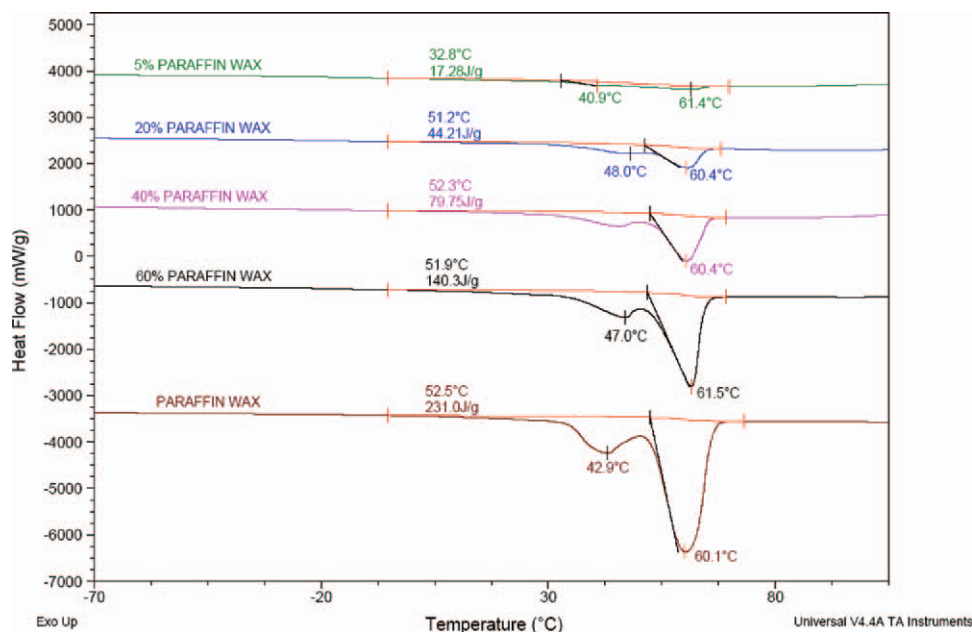
Figure 3. Paraffin/monomer ratio effect on heat storage capacity. [Color figure can be viewed in the online issue, which is available at wileyonlinelibrary.com.]

measured as dried products. SEM micrographs were obtained with a Jeol JSM-5920LV using a secondary electron detector. The samples were investigated with a gold coating in order to allow a contrast imaging of the surfaces. Different regions were analyzed to assure a representative image.

Thermobalance. Thermogravimetric analyses (TGA) were carried out in a SETSYS Evolution-1750 (SETARAM Instruments). The heating rate was 10°C/min in an argon flow rate of 75 mL/min from −70 to 100°C and about 5 mg of sample was used.

RESULTS AND DISCUSSION

Batch Miniemulsion Polymerizations

Figure 1 presents the evolution of the gravimetric monomer conversion for varying amounts of paraffin wax. The formulations are given in Table I. In all cases, complete conversion was reached. It can be seen that not distinction could be made among the kinetics of BM0, BM5, and BM20 due to the fast polymerization rate. However, BM40 and BM60 show a slower polymerization rate. Furthermore, Table II shows that particle size increases as the paraffin wax content increases, the same behavior was reported previously in the literature.[27] The increase in particle size (applying the same energy) as paraffin/monomer ratio increases can be explained taking into account that beside other parameters, it has been reported that the viscosity of the system affects the onset of acoustic cavitation[28] and thus droplet size.

Furthermore, looking at Figure 2, it can be observed that BM0, BM5, and BM20 show narrow PSD and particle size measurement presents only one population (Table II). This suggests that a substantial fraction of the entering droplets was nucleated. However, BM40 and BM60 present broader PSD and dp measurements show two populations (Table II). This could be because secondary nucleation took place (homogeneous or heterogeneous nucleation). For a given formulation, in terms of

monomers, initiators, and surfactants, the probability of new particles formation by homogeneous nucleation increases as the number of particles/droplets in the system decreases.[29,30] In addition, most investigators believe that in the case of partially water-soluble monomers such as MMA, polymer particles are generated by homogeneous nucleation even in the presence of surfactant micelles.[31] Therefore, looking at Table III, it can be said that BM40 and BM60 present homogeneous nucleation, whereas in run BM5 and BM20, the number of particle/droplets was high enough to minimize the homogeneous nucleation. Moreover, it has to be taken into account that this secondary nucleation mechanism is related to the formation of acrylic nanoparticles without PCM inside which could have a negative effect on phase change properties.

Phase Change Properties and Thermal Stability

The latent heat of the encapsulated PCMs was obtained by DSC. Looking at Figure 3, DSC thermograms show that pure paraffin wax melting heat per mass unit is 231 J/g. In addition, it can be observed that as the amount of nanoencapsulated PCM increases latent heat also increases, BM5 (17.28 J/g), BM20 (44.21 J/g), BM40 (79.75 J/g), and BM60 (140.3 J/g).

Table IV. Nanocapsules Latent Heat Capacity and Their Calculated Efficiencies

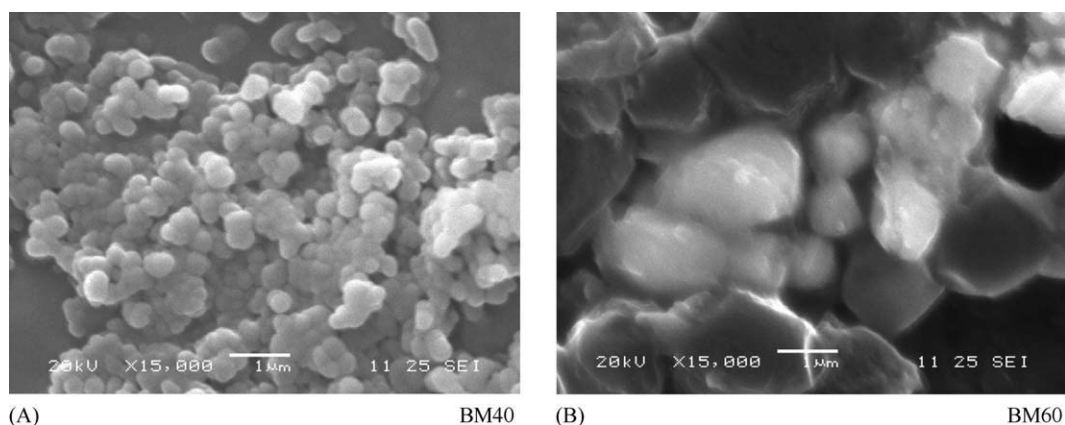| Reference	Enthalpy (J/g)	Encapsulation ratio
Paraffin wax	231	–
BM5	17.20	7.5
BM20	44.21	19.1
BM40	79.75	34.5
BM60	140.3	60.7

Figure 4. SEM image (A) BM40 AND (B) BM60 nanoparticles.

Similar results were achieved by Fang et al.,[22] they concluded that a nanocapsule containing 50 wt % of octadecane present a phase change enthalpy of 124.4 J/g. In the present investigation, the maximum amount of encapsulated PCM achieved was 60 wt %. It was not possible to encapsulate 80 wt % of PCM, the system presented phase separation. Encapsulation ratio was calculated based on paraffin wax enthalpy and nanoencapsulated system enthalpy ratio.[10,16] Table IV shows that the calculated encapsulated ratio is in concordance with the formulations. Moreover, looking to Figure 4, it seems that samples BM40 and BM60 show that all the PCM was encapsulated. However, a deeper study should be carried out to assure that total encapsulation was achieved for all the systems.

Thermal stability was also analyzed. TGA curves for nanocapsules with and without PCM are shown in Figure 5. The TGA of pure paraffin wax shows a market weight loss between 200 and 350°C (Table V). In the case of PMMA (BM0), three degradation steps were observed (Table V):[32–35]

1. First stage: head to head bonds that form by combination termination of two active polymer chains (20–174°C)

2. Second stage: unsaturated end groups that form by disproportionation termination of two active polymer chains (174–327°C)
3. Third stage: random bonds scission of polymer chain (327–450°C)

Nanocapsules show an increase of weight loss between 130 and 350°C as the percentage of encapsulated paraffin was increases (BM5<BM20<BM40<BM60) (Table V). Thermal degradation is controlled by the amount of encapsulated paraffin wax.

Table V. Thermal Properties of Nanocapsules Containing Different Paraffin Wax Concentrations

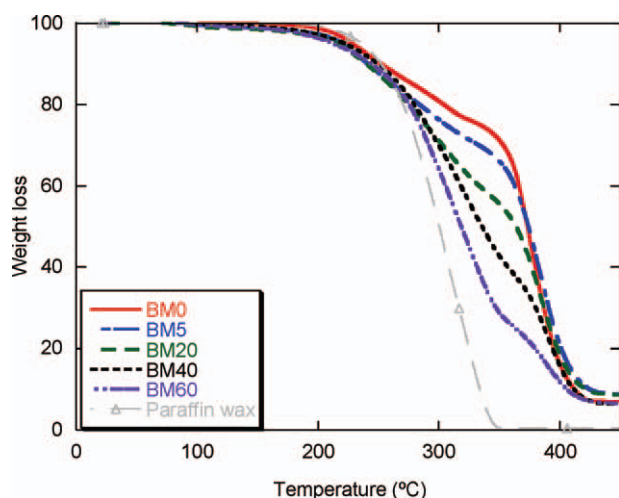| Reference	Degradation interval (°C)	Mass loss (%)
Paraffin wax	179-350	99.6
	Residue	<0.5
BM0	20-174	0.4
	174-327	23.6
	327-450	69.3
	Residue	6.7
BM5	20-130	0.9
	130-329	28.3
	329-450	62.6
	Residue	8.2
BM20	20-130	1.3
	130-340	40.7
	340-450	50.1
	Residue	7.9
BM40	20-124	0.5
	124-358	59.6
	358-450	33.6
	Residue	6.3
BM60	20-135	1
	135-360	73.3
	360-450	20.1
	Residue	5.6

Figure 5. Nanoencapsulation effect on thermal stability. [Color figure can be viewed in the online issue, which is available at wileyonlinelibrary.com.]

Moreover, the encapsulated systems present in all cases a better thermal stability than pure paraffin wax. Even in the case of sample BM60, the one that present the highest paraffin wax concentration, its degradation occurs in a more gradual way than pure paraffin wax.

CONCLUSIONS

Paraffin wax was successfully nanoencapsulated by miniemulsion polymerization technique presenting PMMA as polymeric shell. Stable nanocapsules containing 60 wt % of paraffin wax were synthesized (439.4nm) presenting a heat storage capacity of 140.3 J/g. Systems with higher PCM concentration show phase separation. In the case of nanocapsules containing low amounts of PCM (<20 wt %), droplet nucleation seems to be the main loci of particle formation. However, at higher paraffin wax concentration (40–60 wt %), secondary nucleation takes place. These secondary nucleations must be minimized to avoid the formation of acrylic nanoparticles that could contribute in a negative way in final product heat storage capacity.

Thermal degradation is controlled by the amount of encapsulated paraffin wax. All encapsulated systems present better thermal stability than pure paraffin wax.

REFERENCES

1. Su, J.; Wang, L.-X.; Ren, L. *Colloid Surf. A Physicochem. Eng. Aspects* **2007,** *299*, 268.

2. Hong, Y.; Xinshi, G. *Sol. Energy. Mater. Sol. Cells.* **2000,** *64*, 37.

3. Yamgishi, Y.; Takeuchi, H.; Pyatenko, W.; Kayukawa, N.; *AIChE J.* **1999,** *45*, 696.

4. Hawlader, M. N. A.; Uddin, M. S.; Zhu, H. *J. Int. J. Energy. Res.* **2002,** *26*, 159.

5. Hittle, D. C.; Andre, T. L. *ASHRAE Trans. Res.* **2002,** *108*, 175.

6. Kim, J.; Cho, G. *Text. Res. J.* **2002,** *72*, 1093.

7. Chaurasia, P. *Res. Ind.* **1981,** *26*, 159.

8. Zhang, X.; Pan, Y.; Tao, X.; Yick, K. *Mater. Chem. Phys.* **2004,** *88*, 300.

9. Choi, J.-K.; Lee, J. G.; Kim, J. H.; Yang, H.-S. *J. Ind. Eng. Chem.* **2001,** *7*, 358.

10. Yu, F.; Chen Z.-H.; Zheng X.-R. *Colloid Polym. Sci.* **2009,** *287*, 549.

11. Li, W.; Zhang, X. X.; Wang X.-C.; Niu, J.-J. *Mater. Chem. Phys.* **2007,** *106*, 437.

12. Jin, Z.; Wang, Y.; Liu, J; Yang, Z. *Polymer* **2008,** *49*, 2903.

13. Zhang, H.; Wang, X. *Colloids Surf. A: Physicochem. Eng. Aspects* **1999,** *332*, 129.

14. Liang C.; Lingling, X.; Hongbo, S.; Zhibin, Z. *Energy Conver. Manag.* **2009,** *50*, 723.

15. Sanchez, L.; Sanchez, P.; Carmona, M.; De Lucas, A.; Rodriguez, J. F. *Colloid Polym. Sci.* **2008,** *286*, 1019.

16. Sanchez, L; Rodriguez, J. F.; Romero, A.; Borreguero, A. M.; Carmona, M.; Sanchez, P. *Chem. Eng. J.* **2010,** *157*, 216.

17. Hawlader, M. N. A.; Uddin, M. S.; Khin, M. M. *Appl. Energy* **2003,** *74*, 195.

18. Asua, J. M. *Prog. Polym. Sci.* **2002,** *27*, 1283.

19. Schork, F. J.; Poehlein, G. W.; Wang, S.; Reimers, J.; Rodriguez, J.; Samer, C. *Colloids Surf. A: Physicochem. Eng. Aspects* **1999,** *153*, 39.

20. Landfester, K.; Bechthold, N.; Tiarks, F.; Antonietti, M. *Macromolecules* **1999,** *32*, 5222.

21. Fang, Y; Kuang, S.; Gao, X.; Zhang, Z. *Energy Convers. Manag.* **2008,** *49*, 3704.

22. Fang, Y.; Kuang, S.; Gao, X.; Zhang, Z. *J. Phys. D: Appl. Phys.* **2009,** *42*, 1.

23. Chen, Z.-H.; Zeng, X.-R.; Zhang, Z.-G. *Appl. Energy* **2011,** *91*, 7.

24. Zhang, G. H.; Bon S. A. F.; Zhao, C. Y. *Sol. Energy* **2012,** *86*, 1149.

25. Su, J.; Wang, L.; Ren, L. *J. Appl. Polym. Sci.* **2006,** *102*, 4996.

26. Alkan, C.; Sari, A. *Sol. Energy* **2008,** *82*, 118.

27. Tiarks, F.; Landfester, K.; Antonietti, M. *Langmuir* **2001,** *17*, 908.

28. Briggs, H. B.; Johnson, J. B.; Mason, W. P. *J. Acoust. Soc. Am.* **1947,** *19*, 664.

29. Ferguson, C. J.; Russel, G. T.; Gilbert, R. G. *Polymer* **2002,** *43*, 4557.

30. Rodriguez, R.; Barandiaran, M. J.; Asua, J. M. *Macromolecules* **2007,** *40*, 5735.

31. Nomura, M.; Tobita, H.; Suzuki, K. In Advance in Polymer Science: Polymer Particles; Okubo, M., Ed.; Springer: The Netherlands, **2005;** *Vol 175*, p 27.

32. Grassie, N.; Melville, H. W.; *Discuss Faraday Soc.* **1947,** *2*, 378.

33. Kashiwagi, T.; Hirata, T.; Brown, J. E. *Macromolecules* **1985,** *18*, 131.

34. Hirata, T; Kashiwagi, T.; Brown, J. E. *Macromolecules* **1985,** *18*, 1410.

35. Nising, P.; Zeilmann, T.; Meyer, T. *Chem. Eng. Technol.* **2003,** *26*, 599.